Chall. Nano Micro Scale Sci. Tech., 9(1): 63-68, Winter and Spring 2021
DOI: 10.22111/CNMST.2021.34970.1193

ORIGINAL RESEARCH PAPER

Multi-Objective Optimization of HIV Separation from the Blood Sample Using CFD and NSGA II Algorithm

Mostafa Yousefi[1], Hamed Safikhani[1] , Morteza Yousefi[2], Ali Kamalabadi[3]*

[1]*Department of Mechanical Engineering, Faculty of Engineering, Arak University, Arak 38156-88349, Iran*
[2]*School of Engineering, RMIT University, Melbourne, Australia*
[3]*Department of Mechanical Engineering, Amirkabir University of Technology, 424, Hafez Ave., P.O. Box 1591634311, Tehran, Iran*

Received 8 July 2020; revised 27 January 2021; accepted 27 January 2021 available online 2 September 2021

ABSTRACT: In this study, the Multi-Objective Optimization (MOO) of HIV separation from blood sample in a Lab on a Chip (LOC) is investigated using Computational Fluid Dynamics (CFD) and NSGA algorithm. The separation device consists of two horizontal microchannels separated by a porous layer. The flow is controlled by an infinitesimal channel section connected to one of the microchannels. First, using CFD approach, the fluid flow is studied in over 150 separation devices with different geometrical parameters. All performance parameters like separation efficiency and pressure drop are calculated. Then, already computed numerical results are targeted by a multi-objective genetic algorithm (NSGA II). In optimization process, eight different geometrical and process parameters are considered as optimization variables. Maximum separation efficiency and minimum pressure drop caused by separation are considered as two conflicting optimization objectives. Pareto front is presented to assist the design of the efficient separators. Optimization yielded the optimum configuration of the geometrical and process parameters for the highest efficiency and lowest pressure drop in HIV separation process.

KEYWORDS: *LOC, HIV, CFD, NSGA II, Multi-objective optimization.*

INTRODUCTION

In recent years, the separation of the biological particles suspended in a fluid using microfluidic devices has been both academically and commercially prevalent [1-3]. The diagnosis of HIV illness is a great challenge in many poor countries. The application of LOC seems very promising in view of many researchers due to some advantages like portability, fast diagnostic response and little required sample volume. Since there are enormous kinds of particles in blood, separation of a specific particle in order to diagnose a sickness using a LOC still remains as a baffling challenge. For instance, after being infected by HIV, the number of viruses exponentially increases at the primary stage and reaches to thousands in each micro liter of blood and then increases to a certain stage. However, there exist millions of other particles similar in some properties to HIV in the blood [4, 5]. This causes difficulties for researchers to find reliable methods to gather and separate specific viruses with known properties [6-8]. Generally, the methods to separate particles from blood flow can be divided in two different classes. One is separation based on physical properties of the particles like shape, size, density and electrical or magnetic charge. Although these methods have many advantages, they are not ideal and they also have disadvantages [7-11].

*Corresponding Author Email: *h-safikhani@araku.ac.ir*
Tel.: +989120686211; Note. This manuscript was submitted on July 8, 2020; approved on January 27; published online September 2, 2021.

The second class is associated with using chemicals that are susceptible to make chemical or biological compounds with the desired particle. The disadvantage of this method is its low efficiency.

One strategy to separate viral contaminations from blood, ubiquitously in medicinal industries, is using porous media which can let particles smaller than the size of virus pass [12-16]. However, this method gradually loses its efficiency as pollutions will accumulate over the surface of the porous medium which slows down the passing flow. For improving filtration, blood flow should pass with a tangent velocity so it can clean the porous surface from contaminations, opening up all the porosities. Wang et al. [17] reported that such technique can improve the efficiency of separating viruses in LOCs. They simulated the separation process for different geometrical and process parameters. However, the optimized state and/or the effect of different parameters on performance evaluation were not included. Hypothetically, the optimum performance of the separating machine coincides with maximum separation efficiency and minimum pressure drop. These two targets are conflicting as an increase in one would entice a reduction in the other. In this paper the main goal is to preferably optimize both targets concurrently.

Nomenclature

cp	specific heat capacity
D	mass diffusivity coefficient
Q	heat transfer
t	time
T	temperature
u	velocity in x direction
V	velocity
w	velocity in z direction
x,y	spatial variables
x	vector of input parameters
y	vector of observations

Greek Letters

ε	porosity
λ	thermal conductivity
μ	dynamic viscosity
v	velocity in y direction
ρ	density

Subscripts

a	
f	frost
ef	efficiency

Therefore, taking into account Wang et al. presented model first simulation model was established and validated. then using the multi-objective genetic algorithm design function containing six geometrical and two process variables was optimized to reach desired separation efficiency as well as tolerable pressure drop.

NSGA II is one of the best multi-objective optimization algorithms, first proposed by Deb et al. [18]. It has been successfully applied for many engineering problems and more recently for multi-objective optimization (MOO) of engineering systems [19-24]. Based on the available literature there is no report concentrating on MOO, combining CFD and NSGA II, over HIV separation by a LOC; this is the focus of this study.

MECHANISM OF SEPARATOR OPERATION

The filtration apparatus for HIV separation contains two micro-channels separated by a porous layer. The diameter of the virus is about 120 micron [25] and it is bigger than the 50 micron porosity of the layer and thus no virus can pass the porous layer while blood can get through the layer. So, virus can be separated from the blood medium. Passage of the fluid from the porous layer faces a lot of resistance and as it is depicted from Fig. 1 fluid is likely to pass from the upper micro-channel which has lower resistance and then separation success is very low then. To solve this problem, a channel with a much thinner cross section in comparison with upper micro-channel is placed on the way of fluid. In this state the resistance of both possible pathways is comparable. Ultimately, portion of the fluid would pass from the upper channel while the remaining will get through the lower channel containing the porous layer.

DESIGN VARIABLES AND OBJECTIVE FUNCTIONS

To investigate the possibility of optimizing the performance of the separator, different geometrical parameters as well as porous medium properties and blood velocity entering the separator are considered as optimization design variables. Schematic of geometrical variables is illustrated in Fig. 2 and the range of their variation is listed in Table 1. Objective functions include efficiency and pressure drop of the separator should be favorable maximized and minimized respectively. The separation efficiency and pressure drop functions can be defined according to equations (1) and (2).

$$\eta = \frac{\dot{m}_{purified\ blood}}{\dot{m}_{input\ blood}} \tag{1}$$

$$\Delta P = P_{inlet} - P_{outlet} \tag{2}$$

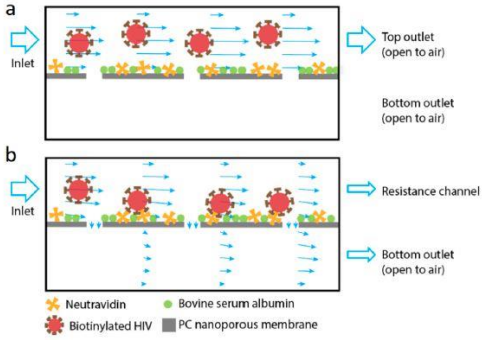

Fig. 1. Schematic of HIV separation device [17].

NUMERICAL MODELING

In this study, the 2D geometry of the separator is considered and after performing mesh sensitivity analysis total number of 54675 hexagonal elements with maximum quality coefficient of 2 is considered.

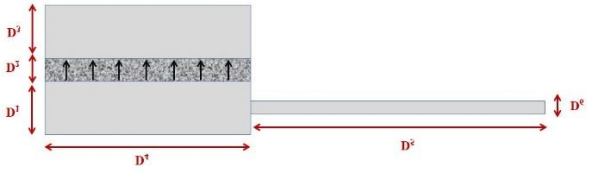

Fig. 2. Geometrical design variables in optimization process.

Table 1
Design variables and their range of variations.

Design Variables	From	To
D_1 *(mm)*	0.05	0.2
D_2 *(mm)*	0.005	0.02
D_3 *(mm)*	0.05	0.2
D_4 *(mm)*	25	45
D_5 *(mm)*	45	85
D_6 *(mm)*	0.01	0.05
D_7=V_i (mm/s)	0.3	3
D_8=K $(1/m^2)$	4.455×10^{17}	5.445×10^{17}

In order to be sure that results would be independent from the selected node grids, different mesh types with different sizes are tested and in each case the optimized network is selected. Mesh sensitivity results are presented in Fig. 3. Figure 4 shows a sample of generated mesh used for optimization. Fluid used in numerical simulation is blood with density of 1060 kg/m3 with viscosity of 0.0035 N.s/m2 in a steady state. The maximum Reynolds number throughout the system is 1.82 which proves that fluid flow is laminar. Governing equations used in numerical simulation include continuity equation, Navier-Stocks and for the porous media Darcy presented in equations (4)-(6) respectively:

$$\frac{\partial(\varepsilon\rho)}{\partial t} + \nabla.(\rho\vec{v}) = 0 \tag{4}$$

$$\frac{\partial(\rho\vec{v})}{\partial t} + \nabla.(\rho\vec{v}\vec{v}) = -\nabla p + \nabla.(\mu\nabla\vec{v}) \tag{5}$$

$$\vec{v} = -\frac{k}{\varepsilon\mu}\nabla p \tag{6}$$

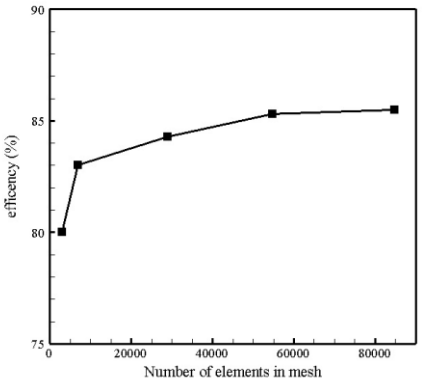

Fig. 3. Results of grid independency test.

One of the boundary conditions is the initial velocity of the fluid into the separator whose variations are listed in Table 1 and the other is the outlet pressure. Boundary conditions are schematically depicted in Fig. 5. For the evaluation purposes, the numerical results from the presented study are compared against experimental data reported elsewhere [29]. As shown in Fig. 6 comparison between numerical results derived here with already reported experimental results, confirms the great correlation with maximum discrepancy of 7%. This error is attributed to the bases for the porous layer in the lower micro-channel which are ignored in numerical models.

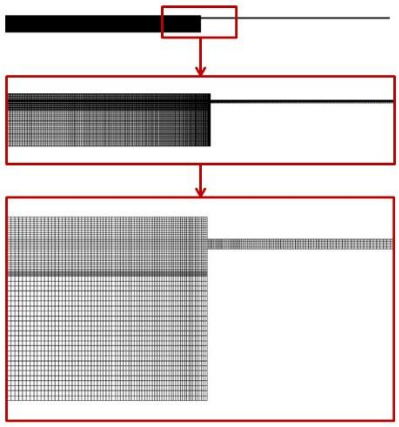

Fig. 4. A sample of generated grid.

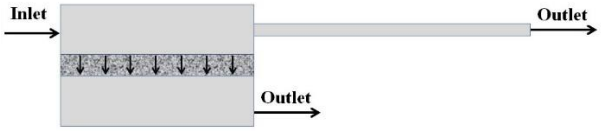

Fig. 5. Schematic of boundary conditions.

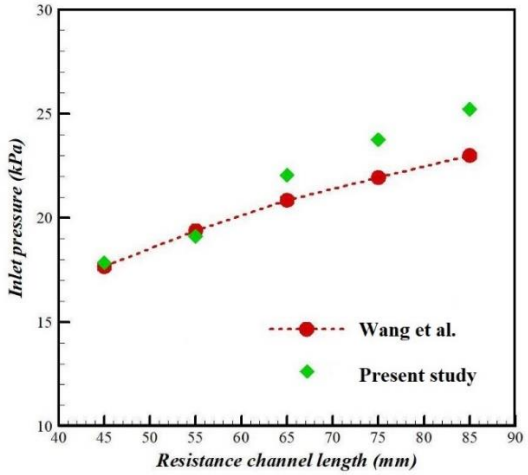

Fig. 6. Validation of the CFD results.

OPTIMIZATION RESULTS

To investigate the optimized performance of the fluid flow in the HIV separators, multi-objective optimization using NSGA II is followed. Population of each generation is considered as 60 while probability of crossover and mutation is selected as 0.7 and 0.07 respectively. Considering the design functions presented in Table 1 and Fig. 2, the optimization can be formulated as presented in equation (7).:

$$Maximize\ \eta = f_1(D_1, D_2, D_3, D_4, D_5, D_6, V_i, K)$$

$$Minimize\ \Delta P = f_1(D_1, D_2, D_3, D_4, D_5, D_6, V_i, K)$$

$$0.05 \le D_1 \le 0.2\ (mm)$$
$$0.005 \le D_2 \le 0.02\ (mm)$$
$$0.05 \le D_3 \le 0.2\ (mm)$$
$$25 \le D_4 \le 45\ (mm)$$

Subjected to: (7)

$$45 \le D_5 \le 85\ (mm)$$
$$0.01 \le D_6 \le 0.05\ (mm)$$
$$0.3 \le D_7 = V_i \le 3\ (mm/s)$$
$$4.455 \times 10^{17} \le D_8 = K \le 5.445 \times 10^{17}$$

In order to cover all variable domain with different combinations of considered parameters 150 different numerical simulations are performed. Fig. 7 and Table 2 contain some of the simulation results. Fig. 8 shows the Pareto front of two objective functions.

As can be seen from the Pareto diagram there is no preference in the domain as moving from one point to another point means a guaranteed change in both objective functions in the way that one is increased and another is decreased. Considering the Pareto front there are three optimum points *A*, *B* and *C* whose data is presented in Table 3.

Aforementioned points in Fig. 8 possess unique properties. Points *A* and *C* are associated with minimal pressure drop and maximal separation efficiency. The ideal point is the one at which both objectives are satisfactorily met. To specify such point mapping method is used [25]. Therefore, both objective functions are varied in the range of 0 to 1 and the norms are depicted. Ideal design point is the one with maximum norm value. Point *B* is the point elicited using such method that partially satisfies both objective functions.

Figure 9 shows the velocity contour at the initial, middle and outlet planes throughout the separator of *B* optimal point. It is noteworthy to compare 150 sets of data resulted from the CFD with Pareto front. Fig. 10 shows the correspondence of the Pareto front and initial CFD data. From this diagram it can be inferred that Pareto front successfully detected the best evolution of the CFD data in terms of lowering the pressure drop and soaring the separation efficiency.

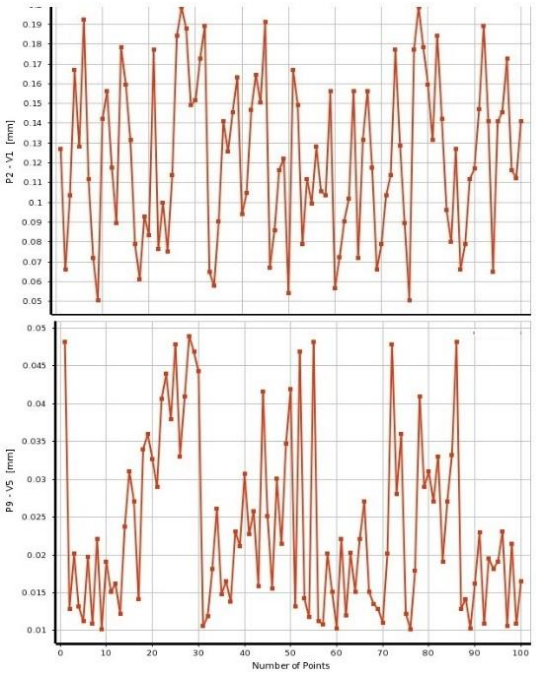

Fig. 7. Part of 150 CFD runs.

Table 2
Samples of numerical results using CFD

Num	Design Variables								Objective Functions	
	D1 (mm)	D2 (mm)	D3 (mm)	D4 (mm)	D5 (mm)	D6 (mm)	V_i (mm/s)	K*10^{-17} (m^{-2})	η (%)	ΔP (pa)
1	0.10	0.010	0. 10	35.0	65.0	0.020	2.40	4.95	40%	47578
2	0.05	0.005	0.05	25.1	45.2	0.010	0.31	4.46	84%	4321
3	0.06	0.008	0.15	29.3	59.6	0.047	1.20	4.70	5.5%	3253
4	0.17	0.020	0.10	30.3	53.5	0.025	0.34	4.99	10%	6819
5	0.09	0.006	0.07	32.3	56.7	0.022	2.42	4.58	42%	26225
6	0.16	0.011	0.12	34.3	59.9	0.019	1.81	5.17	38%	63758
7	0.12	0.017	0.18	36.9	79.4	0.026	1.83	4.94	18%	31230
8	0.19	0.009	0.15	38.9	82.6	0.023	1.22	4.53	42%	36051
9	0.11	0.015	0.19	40.9	78.2	0.019	0.62	5.11	38%	16495
10	0.17	0.018	0.14	42.9	81.4	0.016	2.69	4.71	50%	168840
…										
150	0.18	0.014	0.09	38.3	79.1	0.015	0.6	5.34	58%	44698

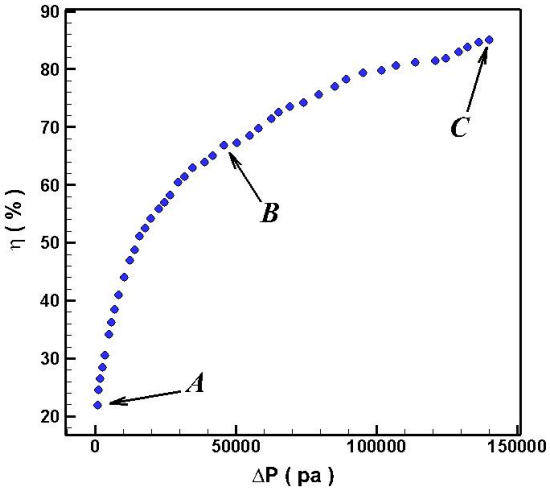

Fig. 8. Pareto front.

Table 3
The values of objective functions and their associated design variables of the

Point	Design Variables								Objective Functions	
	D_1 (mm)	D_2 (mm)	D_3 (mm)	D_4 (mm)	D_5 (mm)	D_6 (mm)	V_i (mm/s)	$K*10^{-17}$ (m^2)	η (%)	ΔP (pa)
A	0.10	0.005	0.1	38.1	50.64	0.048	0.00039	5.28	22.6	748
B	0.20	0.005	0.1	43.1	50.96	0.020	0.0029	4.76	68.8	54722
C	0.17	0.012	0.1	36.1	67.12	0.011	0.0021	4.76	85.3	139805

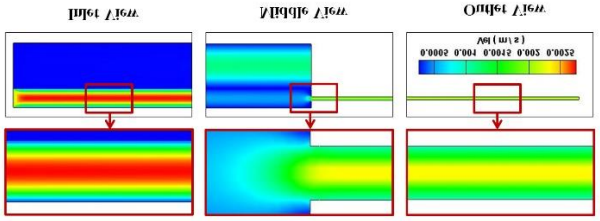

Fig. 9. The velocity contour at the initial, middle and outlet planes of *B* optimal point

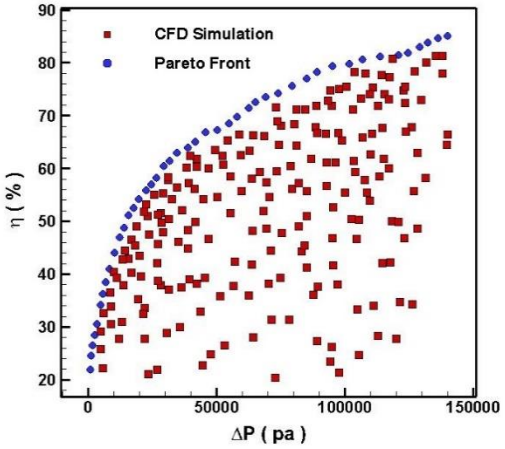

Fig. 10. Overlay of the CFD and Pareto data.

This validates the process of MOO presented in this study. All three selected points are validated by CFD analysis and results are listed in Table 4. Values reveal the error less than 1% which firmly proves the accuracy of the multi-objective optimization process presented here.

Table 4
Re-evaluation of the obtained optimal Pareto front using numerical method.

Point	η (%)			ΔP (pa)		
	Optimization	Numerical	Error (%)	Optimization	Numerical	Error (%)
A	22.6	22.75	0.7	748	750.25	0.3
B	68.8	69.35	0.8	54722	54341	-0.7
C	85.3	85.55	0.3	139805	141074	0.9

CONCLUSION

In this paper, MOO of fluid flow within a LOC for HIV separation from blood sample was concentrated using CFD and NSGA II Algorithm. The main goal was to simultaneously minimize and maximize two conflicting objectives of pressure drop and separation efficiency. Separator possesses two micro-channels with a porous layer between them. The flow was controlled by containing a narrow channel into one of the micro-channels. First, 150 CFD simulations with different geometrical and process parameters were performed and separation efficiency and pressure drop were computed. Then, numerical results were used in a multi-objective optimization model. Design variable of the optimization model were eight parameters including geometry of channels, input velocity to the separator and diffusive coefficient of the porous layer while separation efficiency and pressure drop was the optimization objectives. Pareto front, containing foremost data for designing the separators were also presented and finally optimum combination of the parameters leading to satisfactory optimization outputs were analyzed and discussed.

REFERENCES

[1] Chin CD, Laksanasopin T, Cheung YK, Steinmiller D, Linder V, Parsa H, Wang J, Moore H, Rouse R, Umviligihozo G. Microfluidics-based diagnostics of infectious diseases in the developing world, Nature medicine, Vol. 17, No. 8, pp. 1015, 2011.

[2] Chin CD, Linder V, Sia SK. Lab-on-a-chip devices for global health: Past studies and future opportunities, Lab on a Chip, Vol. 7, No. 1, pp. 41-57, 2007.

[3] Damhorst GL, Watkins NN, Bashir R. Micro- and nanotechnology for HIV/AIDS diagnostics in resource-limited settings, IEEE Transactions on Biomedical Engineering, Vol. 60, No. 3, pp. 715-726, 2013.

[4] Raposo G, Stoorvogel W. Extracellular vesicles: exosomes, microvesicles, and friends, Journal of Cell Biology, Vol. 200, No. 4, pp. 373-383, 2013.

[5] Ribeiro RM, Qin L, Chavez LL, Li D, Self SG, Perelson AS. Estimation of the initial viral growth rate and basic reproductive number during acute HIV-1 infection, Journal of virology, Vol. 84, No. 12, pp. 6096-6102, 2010.

[6] Andersson H, Van den Berg A. Microfluidic devices for cellomics: a review, Sensors and actuators B: Chemical, Vol. 92, No. 3, pp. 315-325, 2003.

[7] Pamme N. Continuous flow separations in microfluidic devices, Lab on a Chip, Vol. 7, No. 12, pp. 1644-1659, 2007.

[8] Sajeesh P, Sen AK. Particle separation and sorting in microfluidic devices: a review, Microfluidics and nanofluidics, Vol. 17, No. 1, pp. 1-52, 2014.

[9] Lenshof A, Laurell T. Continuous separation of cells and particles in microfluidic systems,

Chemical Society Reviews, Vol. 39, No. 3, pp. 1203-1217, 2010.

[10] McGrath J, Jimenez M, Bridle H. Deterministic lateral displacement for particle separation: a review, Lab on a Chip, Vol. 14, No. 21, pp. 4139-4158, 2014.

[11] Xi HD, Zheng H, Guo W, Gañán-Calvo AM, Ai Y, Tsao CW, Zhou J, Li W, Huang Y, Nguyen NT. Active droplet sorting in microfluidics: a review, Lab on a Chip, Vol. 17, No. 5, pp. 751-771, 2017.

[12] Chen X, Liu CC, Li H. Microfluidic chip for blood cell separation and collection based on crossflow filtration, Sensors and Actuators B: Chemical, Vol. 130, No. 1, pp. 216-221, 2008.

[13] Li X, Chen W, Liu G, Lu W, Fu J. Continuous-flow microfluidic blood cell sorting for unprocessed whole blood using surface-micromachined microfiltration membranes, Lab on a Chip, Vol. 14, No. 14, pp. 2565-2575, 2014.

[14] VanDelinder V, Groisman A. Separation of plasma from whole human blood in a continuous cross-flow in a molded microfluidic device, Analytical chemistry, Vol. 78, No. 11, pp. 3765-3771, 2006.

[15] VanDelinder V, Groisman A. Perfusion in microfluidic cross-flow: separation of white blood cells from whole blood and exchange of medium in a continuous flow, Analytical Chemistry, Vol. 79, No. 5, pp. 2023-2030, 2007.

[16] Wickramasinghe S, Kalbfuss B, Zimmermann A, Thom V, Reichl U. Tangential flow microfiltration and ultrafiltration for human influenza A virus concentration and purification, Biotechnology and bioengineering, Vol. 92, No. 2, pp. 199-208, 2005.